NC STATE
Wilson College of Textiles

JTATM
Journal of Textile and Apparel, Technology and Management

Special Issue: 2022

Investigation of Role of Cell Geometry on Compression Behavior of 3-D Woven Hemp Honeycomb Composites

Omender, Zunjarrao Kamble, and B.K. Behera
Department of Textile and Fibre Engineering,
Indian Institute of Technology Delhi
India

ABSTRACT

This research aims to develop a 3D woven honeycomb preform using hemp and Kevlar yarn. Hemp and Kevlar honeycomb preforms with four different cell sizes were developed on a customized weaving machine with multiple beam arrangements. The cell size was varied by changing the number of picks in the free/bonded wall of the honeycomb. The honeycomb composites were developed using the vacuum bagging technique. The quasi-static flatwise compressive strength of the sandwich honeycomb composites was investigated. It was observed that the specific compressive strength of the hemp and Kevlar composite increases with a decrease in cell size. Similarly, the strain energy per unit volume increases with a decrease in cell size. The compressive strength and strain energy per unit volume decrease with an increase in core height.

Keywords: 3-D woven honeycomb fabrics; Composites; Vacuum bagging; energy absorbing structures

1. Introduction

Lightweight engineering seeks novel ways to make products lighter without weakening them, and in some cases, even strengthening them. One option is to use cellular structures and materials, such as honeycombs, as a solution for lighter items. However, honeycomb structures are frequently employed as sandwich panels in various applications due to their outstanding mechanical qualities (high stiffness) and energy absorbing capacity [1–3]. Honeycomb cores with hexagonal structures provide stronger shear rigidity, higher crushing stress, extended stroke, low weight, and continuous crushing force in sandwich panels [4,5]. The hollow gaps save weight while simultaneously ensuring essential strength. Due to their unique qualities resulting from their cellular architectures, cellular solids like sandwich panels have been employed as sophisticated materials in the aerospace, automobile, and marine sectors for decades [6,7]. Due to its hollow core structure, woven textile reinforced honeycomb composite can be considered a cellular solid and a new product in the family of lightweight energy absorbent materials. In recent years, there has been a lot of interest in figuring out how to weave this intricate structure and how it performs mechanically under various loads [8,9].

Most of the literature reported that the honeycomb sandwich panels are related to polymeric and metal honeycombs and only a few studies have demonstrated 3D woven honeycomb preforms and their composites. 3D woven honeycomb fabrics are structures with multiple fabric layers integrated by weaving together warp or weft yarns of adjacent fabric layers at a particular position [10]. It has been reported that the compression strength of polymeric honeycomb sandwich panel changes with cell size [11,12], and the compressive strength and energy increases with a decrease in cell size [13–15]. Further, filling the empty cells of the honeycomb with foam-like material enhances compression strength and energy absorbed. Oblique/inclined loads in compression and energy absorption characteristics in Plascore Nomex honeycomb core under dynamic and static loading are also investigated. To change the direction of the cell wall for load inclination, core specimens were placed off-axis. The goal of the research was to see how core thickness, loading angle, and test speed affected energy absorption. At velocities of 10 mm/min, 30, 60, 100, and 120 m/s, honeycomb specimens with the cubical structure were evaluated with and without a face sheet. For two types of honeycombs, the mean crushing force was calculated using varied impact velocities [16]. A study was conducted on the augmentation of strength due to the built-in air pressure in the honeycomb cell wall. During dynamic crushing, it was discovered that entrapped air in honeycomb induces strain hardening [17].

The peak and mean collapse loads, as well as the energy absorbed during paper honeycomb crushing, are influenced by the loading rate. The rate dependency of the core materials affects the mean crushing stress, peak crushing stress, and energy absorbed per unit volume of the core. The amount of energy absorbed by compressed cores grows in lockstep with the specimen's volume. When the number of layers is doubled (double or triple layer) rather than employing a single layer, the total energy absorbed increases two to three times [18]. When the honeycomb is loaded in-plane, the cell walls bend first, followed by linear elastic deformation. Gibson and Ashby [19] developed a link between Young's modulus and cell geometrical parameters such as cell wall length, cell wall thickness, and cell opening angle of honeycomb under linear elastic deformation. The mechanical performance of the honeycomb changes with cell shape. The strength of square honeycombs is 27% more than that of triangular honeycombs and other core shapes [20].

Researchers have developed a variety of recyclable materials based on natural fibers such as flax, hemp, kenaf, jute, oil palm, coconut, and many more in response to growing environmental concerns. Natural fibers are low-cost materials with low density, high specific qualities, biodegradable, and can be recycled [21–23]. Many studies have demonstrated that composites made of natural fibers can have qualities comparable to those made of conventional fibers if properly developed. The natural fiber reinforced composites are environmentally friendly and economical. Therefore, 3D woven honeycomb fabrics were developed using hemp and Kevlar yarns in this study. 3D woven honeycomb fabrics with four different cell sizes were developed. Their composites were characterized for flatwise compression strength. The effect of core height was also investigated.

2. Materials and methods

2.1 Materials

The spun hemp yarn having linear density 105 tex and Kevlar yarn having 66.6 tex was used to produce the 3D woven honeycomb preforms. The hemp yarn was procured from the local market in New Delhi, India, and the Kevlar yarn was kindly donated by Arvind advanced materials, India. Epoxy resin (ARL 125) and its curing agent (AH 360), supplied by Atul Ltd., were used as a matrix material to manufacture the composites.

2.2 Methods

2.2.1 Weaving of 3D Honeycomb preform

The 3D honeycomb preforms were woven using the principle of double cloth weaving on a sample weaving machine having creel to accommodate four beams. The 3D woven honeycomb preforms were developed with 3, 5, 7, and 9 picks in their free (l_f) and bonded wall (l_b) (Figure 1a). Generally, the honeycomb fabric is coded as (x,y)PzLθ. Where x and y are a number of picks (P) in the free and bonded wall (when x and y are the same, then it is represented by a single number), z denotes the number of fabric layers (L), and θ is the cell opening angle [24]. The cross-sectional representation of developed honeycomb preforms is shown in Figure 1 (b-e). Geometric details of the woven honeycomb structures are depicted in Table 1. Here, all four different preforms have the same weaving specifications except the number of picks in the free and bonded wall. Therefore the areal density of all the hemp preforms was maintained at 820 ± 11 grams per square meter and that of Kevlar at 520 ± 6 grams per square meter. The plain weave hemp and Kevlar fabrics with twenty ends and picks per meter were developed to produce composite skin for the honeycomb sandwich panel.

Table 1. Details of 3D woven honeycomb composite structures (warp and weft linear density = 105 tex; Number of fabric layers = 7; Number of sections = 4; Ends and picks per meter = 788; Opening angle = 60^0).

Specimen ID	Length of free/bonded wall (mm)	Cell height (mm)	Face sheet thickness (mm)
3P4L60	3.8	6.6	1 ± 0.05
5P4L60	6.4	10.9	
7P4L60	8.9	15.4	
9P4L60	11.4	19.8	

2.2.2 Theoretical analysis of areal density of 3D woven honeycomb fabric

The determination of the theoretical areal density of the 3D woven honeycomb fabric before actual preform weaving is essential to design the composite component of desired mass density. To the best of our knowledge, there is no reported attempt to estimate the theoretical areal density of 3D woven honeycomb preform. The modified approach to determine fiber volume fraction of 3D woven honeycomb is reported by Tripathi et al [24]. By extending the geometric model reported by Tripathi et al, the model for areal density is derived. Different steps to arrive at an areal density (equation 1) of 3D woven honeycomb preform are shown below.

$$\text{Total number of sections per meter} = \frac{100}{2(l_f + w)} \quad (1)$$

$$\text{From Figure 1(a), } w = l_f \cos\theta \quad (2)$$

$$\text{Length of warp yarn in } q^{th} \text{ section of } p^{th} \text{ layer} = \frac{Q_{pq}}{V_{pq}}(1 + H_{1pq}) \quad (3)$$

Total length of warp yarn in one meter= $\dfrac{100}{2(l_f + w)} \dfrac{Q_{pq}}{V_{pq}} (1 + H_{1pq}) \times EPM \times P$ (4)

Weight of warp per meter = $\dfrac{100}{2(l_f + w)} \dfrac{Q_{pq}}{V_{pq}} (1 + H_{1pq}) \times EPM \times P \times \lambda_p$ (5)

Total length of weft per meter = $100 * (1 + H_{2pq}) \times Q_{pq} \times P \times \dfrac{100}{2(l_f + w)}$ (6)

Weight of weft per meter = $100 * (1 + H_{2pq}) \times Q_{pq} \times P \times \dfrac{100}{2(l_f + w)} \times \mu_{pq}$ (7)

Areal density (Grams per sq meter) of 3D woven honeycomb =

$$\frac{Q_{pq} P}{2(l_f + w)} \left[\left(\frac{(1 + H_{1pq}) \cdot EPM \cdot \lambda_p}{V_{pq}} \right) + \left((1 + H_{2pq}) \cdot \mu_{pq} \right) \right] \quad (8)$$

Where, Q_{pq} is the number of picks in q th section of p th layer of honeycomb fabric, EPM ends per meter, and P is the number of layers, H_{1pq} and H_{2pq} is Crimp in warp and weft yarn in q th section of p th layer of honeycomb fabric, respectively, λ_p is warp yarn linear density, V_{pq} is pick per unit length of q th section in p th layer of honeycomb fabric, μ_{pq} is weft yarn linear density.

2.2.3 Development of 3D woven honeycomb composites and their sandwich panels

The stainless steel molds of appropriate size and shape were fabricated. The molds were coated with wax to facilitate easy removal. The molds were inserted into the hollow channels within the preform. The resin was then applied to the fabric. The preform impregnated with resin was then placed into the vacuum bag to force out the excess resin. The composite was then allowed to cure inside the vacuum bag at room temperature for twenty-four hours. The composite development process is shown in Figure 2. The plain weave hemp fabric was converted to composite using a vacuum-assisted resin infusion technique. This plain-woven hemp composite was used as the skin of the honeycomb sandwich.

2.2.4 Characterization of the composite specimens

The developed composites were characterized for flatwise compressional properties using ASTM C365/C365M standards. The honeycomb specimens with nine cells for each type of composites were used. The core height was maintained at 20 mm. The specimen size used are shown in Table 2. To investigate the effect of core height, four different core heights, namely: 10, 20, 25, and 30 mm, were chosen. The plain-woven hemp fabric composite was used as face sheet material. The face sheet was pasted to a honeycomb using Araldite rapid curing epoxy resin.

Table 2. Specimen size used for flatwise compression test

Specimen ID	3P4L60	5P4L60	7P4L60	9P4L60
Size (mm × mm)	16.5 × 15.5	26 × 26	40 × 40	48 × 48

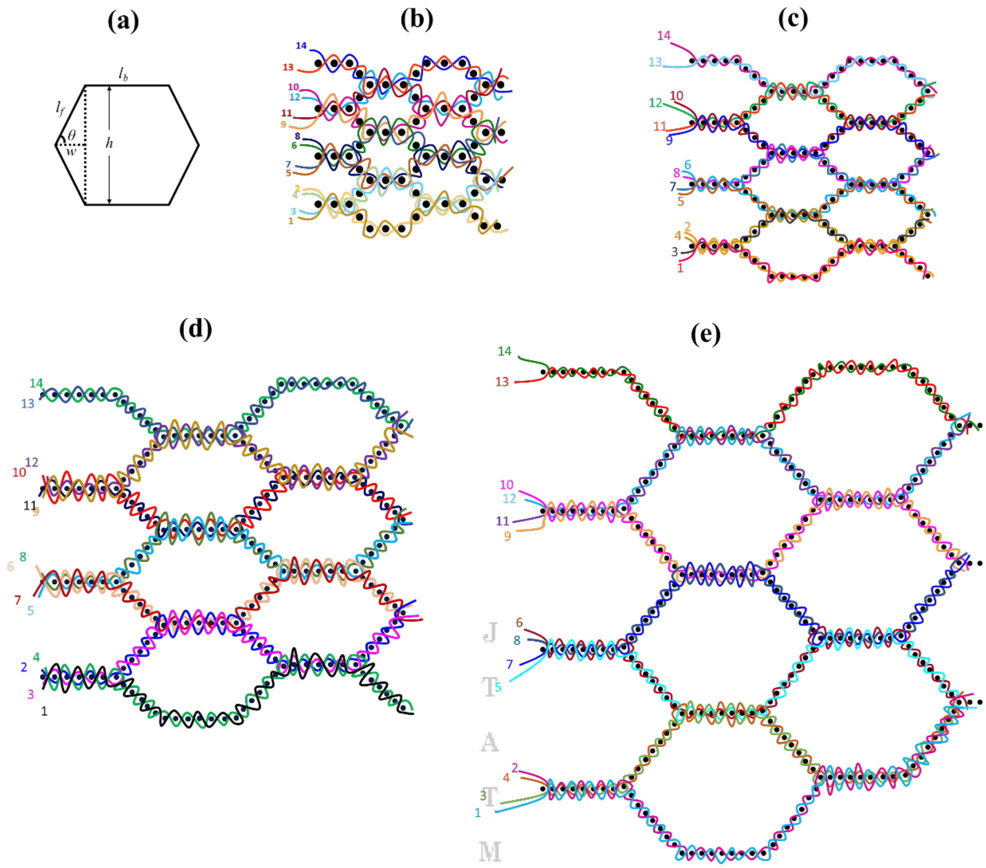

Figure 1. Geometry of a cross-section of the unit cell of the honeycomb fabric (a), Cross-sectional representation of 3D woven honeycomb preforms with 3 (b), 5 (c), 7 (d), and 9 (e) picks in their free and bonded walls.

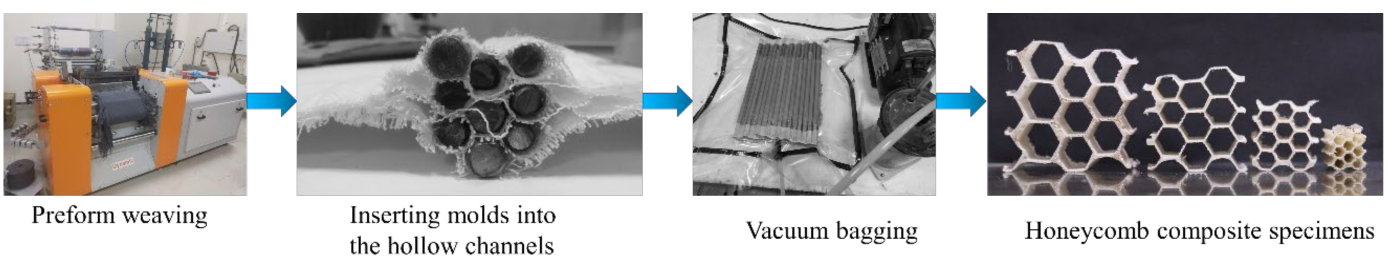

Figure 2. 3D woven honeycomb composite development process.

3. Results and discussion

3.1 Comparative analysis of predicted and experimental areal density of 3D woven honeycomb

The areal density of the 3D woven hemp honeycomb fabrics was estimated using the developed geometric model, and the obtained values were compared with experimental values. Five fabric samples having the size $10 \times 10\ cm^2$ were taken and weighed. The estimated and experimental data error was calculated and shown in Figure 3. Good agreement was observed between the experimental and predicted areal density of both the hemp and Kevlar honeycomb fabrics.

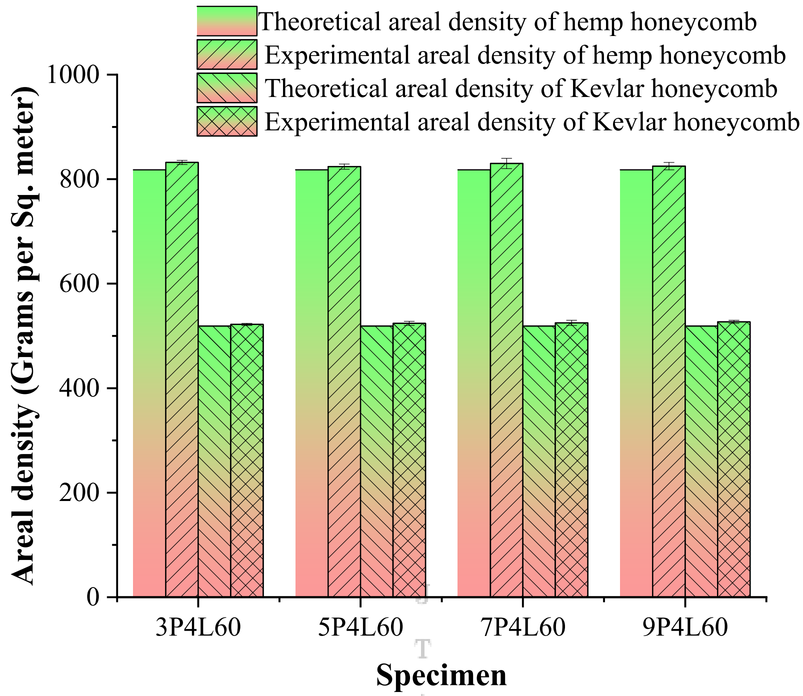

Figure 3. Comparison of theoretical and experimental areal density

3.2 Influence of cell size on compressive properties of honeycomb composites

Figure 5a shows the maximum compressive loads of hemp honeycomb composites with varying cell sizes. The compressive strength of hemp honeycomb composite specimen having 5-, 7-, and 9-mm cell size is ~72, ~177, and 264% higher than composite with 3 mm cell size. The higher compressive strength for honeycomb composite 9P4L60 is due to the longer wall length, which takes part in load-bearing [25]. It can be explained further as the free or bonded wall-length increases, the cells and foil edge area per unit honeycomb surface area decreases (Equation 2 and 3). The equation 2 and 3 were calculated from grometric relationships within the honeycomb unit cell shown in Figure 4 [26]. However, each honeycomb composite sample having nine cells was tested for compression. Therefore, the value of C is the same for all four specimens. Although the foil edge area decreases with an increase in free wall length, however, nine cells were tested for compression for each specimen, the F_a is relatively higher for specimen having longer free/bonded wall length. The foil edge area of different honeycomb composite specimens tested in this study is shown in Table 3. The same trend was observed for 3D woven Kevlar composites. The compressive strength of the Kevlar honeycomb composite specimen having 5-, 7-, and 9-mm cell sizes is ~125, 298, and 532% higher than composite with 3 mm cell size. The compressive strength of Kevlar composites with varying number picks in free and bonded wall area is shown in Figure 5a.

$$Cells\ per\ honeycomb\ surface\ area\ (C) = \frac{1}{(l_b + l_f cos\theta)(2l_f sin\theta)} = \frac{1}{2.6 l_b^2} \qquad (9)$$

$$Foil\ edge\ area\ per\ honeycomb\ surface\ area\ (F_a) = \frac{(l_b t_b + l_f t_f)}{(l_b + l_f cos\theta)(2 l_f sin\theta)} = \frac{1.54}{l_b} \quad (10)$$

Table 3. Foil edge area of different honeycomb composite specimens

Specimen	Foil edge area of nine honeycomb cells (mm^2)
3P4L60	60.8
5P4L60	96.9
7P4L60	138.7
9P4L60	174.8

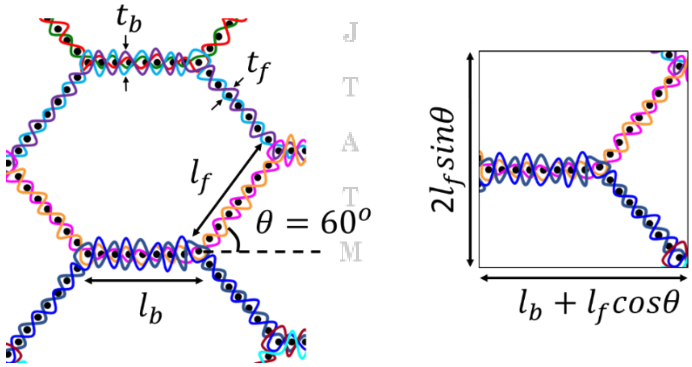

Figure 4. Various geometric parameters of a honeycomb unit cell

The specimens tested for compressive strength have nine cells each. However, the sizes of different honeycomb composites were different. Therefore, the specific compressive strength of different composite specimens was determined by normalizing with specimen mass, which was calculated using the equation below.

$$Pspec = \frac{Pmax}{m}$$

Where P_{spec} indicates mass-specific compressive strength, P_{max} is maximum compressive strength, and *m* is specimen mass. It has been observed that the specific compressive strength of the hemp honeycomb composites was in the order of 3P4L60 > 5P4L60 > 7P4L60 > 9P4L60. The higher specific compressive strength of 3P4L60 is due to lower specimen size and thereby lower weight. The results are shown in Figure 5c. The compressive strength of Kevlar composites is lower than hemp composites. However, the specific compressive strength (compressive strength per unit weight) is higher than equivalent hemp honeycomb composites. This is attributed to the lower density of Kevlar compared to hemp fiber.

Although the effect of the composite specimen's mass is taken into account in the specific compressive strength, due to their vastly differing volumes, it may not be a realistic representation of their performance under compressive load. From the load-deformation curves, the strain energy up to maximum compressive load (first peak load) was determined, and the data were normalized with the volume of the corresponding specimen. The results are shown in Figure 6a. The specific strain energy of different hemp and Kevlar honeycomb composites was found in the same order as specific compressive strength (Figure 6b). However, the specific strain energy of Kevlar honeycomb composites was lower than equivalent hemp honeycomb composites. This is again attributed to the lower density of Kevlar fiber compared to hemp. The Specific strain energy of Kevlar honeycomb composites with 3, 5, 7, and 9 picks in their free and bonded wall was ~11, ~27, ~24, and ~28% higher than equivalent hemp honeycomb composites.

3.3 Influence of core height on compressive properties of honeycomb composites

Figure 5b shows the compressive load experience by a hemp honeycomb composite with varying core height. It has been observed that with an increase in core height from 10 mm to 20 mm, the compressive strength of the honeycomb composite increases by ~116%. However, for core heights of 25 and 30 mm, a decrease in the increment of the compressive strength was observed. This may be due to the early buckling of the honeycomb cell wall. The specific compressive strength of the composites decreases with an increase in core height (Figure 5d). Similarly, the specific strain energy also decreases with an increase in core height. Further, the increased free/bonded wall-length decreases the exposed foil area per unit honeycomb volume decreases the specific strain energy. The exposed foil area is be calculated from equation 4 [26]

$$Exposed\ foil\ area\ per\ honeycomb\ volume = \frac{2\left(l_b + 2l_f\right)}{(l_b + l_f cos\theta)(2l_f sin\theta)} = \frac{15.6}{l_b} \qquad (11)$$

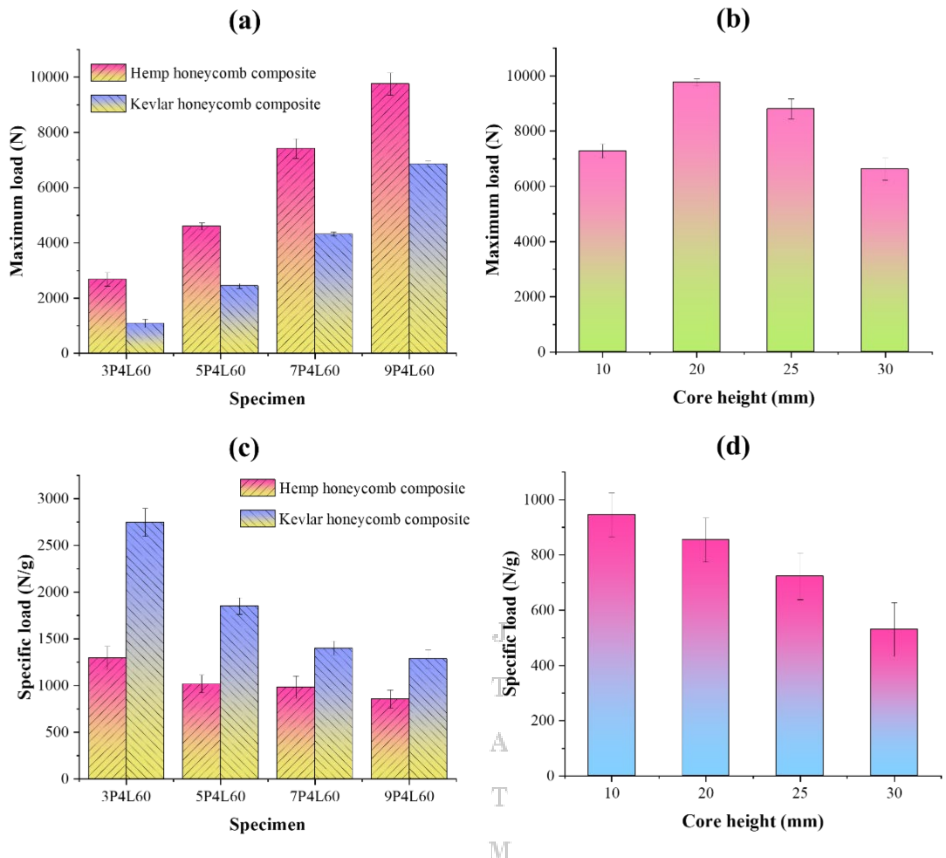

Figure 5. Flat wise compressive strength of different honeycomb composites (a), Flat wise compressive strength of hemp honeycomb composites with different core heights (b), Specific compressive strength of different honeycomb composites (c), Specific compressive strength of hemp honeycomb composites with different core heights (d).

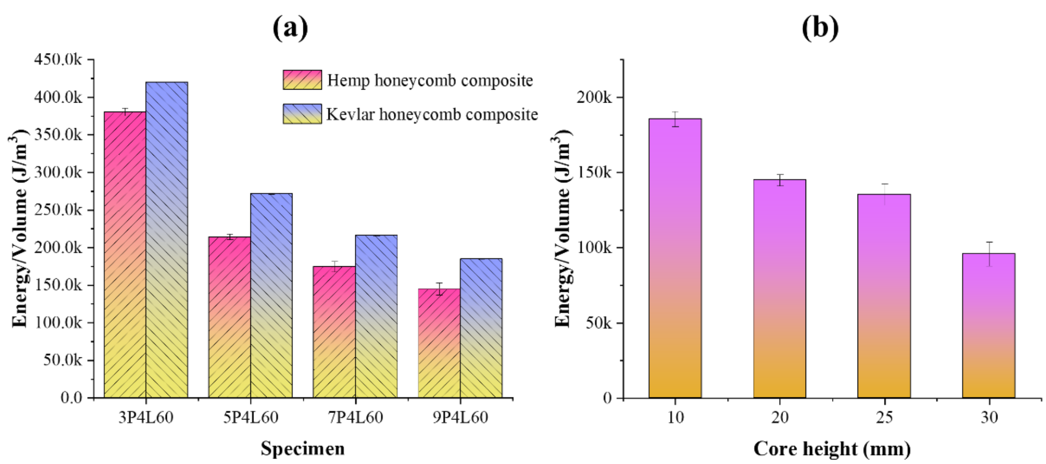

Figure 6. Strain energy per unit volume for different honeycomb composites (a) and honeycomb composites with different core heights (b).

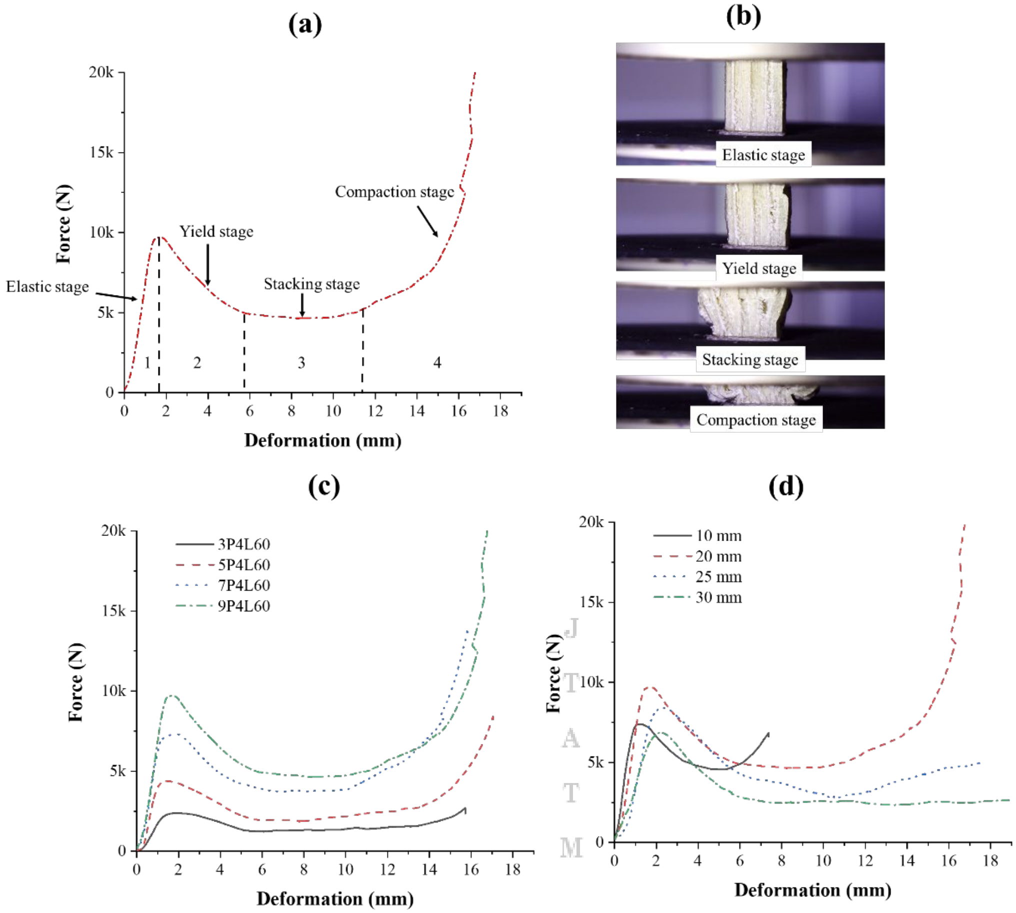

Figure 7. Stages of failure for honeycomb composites (a, b), Load-deformation curves for different hemp honeycomb composites (c), and hemp honeycomb composites with different core heights (d).

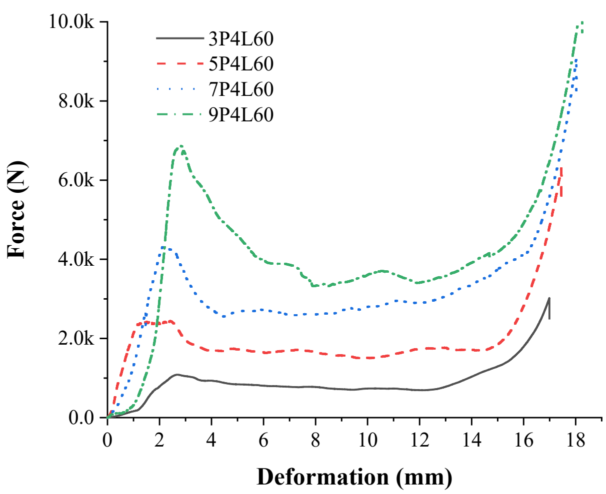

Figure 8. Load-deformation curves for different Kevlar honeycomb composites.

3.4 Failure modes of honeycomb composites in compression

The load-deformation curves of hemp honeycomb composites are shown in Figure 7 (a and c). It must be understood that the peak stress experienced by the composites was calculated by considering the total area of the structure, including the area between the hollow spaces. The load-deformation curves can be divided into four stages. The first stage is an elastic stage, in which the honeycomb composite deforms elastically until it reaches the peak load. The peak load increase with an increase in cell size. The yield stage corresponds to elastic buckling of the walls, which causes a gradual reduction in the load experienced by the composite. This follows the long deformation plateau region within which the composite experience nearly the same load. The length of this region exhibits the energy absorption capability of that composite material. Interestingly, the length of this region in all the composite was found nearly the same for composite with different cell sizes. Eventually, the densification of the composite causes compaction of the structure and complete failure. The plateau region for different composites was found nearly the same. This indicates that the plateau region is independent of cell size. The Kevlar composites also show a trend similar to hemp honeycomb composites (Figure 8). However, the stacking region is slightly higher in Kevlar honeycomb composites than hemp composites. Figure 7d shows the load-deformation curves of hemp honeycomb composites with varying core heights. It can be seen that the plateau region increases with an increase in core height. The honeycomb composite with less core height reaches the stacking stage earlier.

3.5 Comparative analysis of developed honeycomb composites with reported studies

Bang and Cho [27] reported compression properties of aluminium 3104 honeycomb having wall thickness 0.05 mm and cell size 6.35 mm and core height 18 mm. The compressive strength of aluminium honeycomb was ~4500 N. They did not reported the tested specimen dimensions. Li and Ma [28] reported the compressive strength of Nomex honeycomb (3.2 mm cell size) with basalt fabric face sheet and core height of 15 mm as ~4500 N and the specific compressive strength of 0.1 N/mm3. The compressive strength of the 3D woven Kevlar honeycomb with cell size 5 mm and core height 18 mm developed in this study is 3192 N, and the specific compressive strength is 0.47 N/mm3. The specific strength of 5 mm cell size Kevlar honeycomb is ~370% higher than Nomex honeycomb of 3.2 mm cell size.

4. Conclusions

This study reported the compressive performance of 3D woven hemp and Kevlar honeycomb composites. The results indicate that the compressive strength of hemp and Kevlar honeycomb composites increases with a decrease in cell size. Similarly, the specific strain energy per unit volume of hemp and Kevlar honeycomb composites increases with a decrease in cell size. The compressive strength notably changes with honeycomb core height. The results of this study can be used to design and develop natural fiber-based honeycomb composite sandwich panels for a range of applications. The future scope of this research could be investigating the role of filler such as auxetic foam and hybrid structures such as honeycomb-corrugated hybrid sandwich structures on the compressive strength of the materials.

References

1. Tripathi, L.; Behera, B.K. Review: 3D woven honeycomb composites. *J. Mater. Sci.* **2021**, *56*, 15609–15652, doi:10.1007/s10853-021-06302-5.
2. Domb, R.; Jadhav, S.; Gajare, S.; Kadam, N.; Yadav, P.A.B. Design of Honeycomb Sandwich Panel and Its Validation with Flooring Plate of Bus. **2018**, 490–495.

3. Sypeck, D.J.; Wadley, H.N.G. Cellular Metal Truss Core Sandwich Structures. *Adv. Eng. Mater.* **2002**, *4*, 759–764, doi:10.1002/1527-2648(20021014)4:10<759::AID-ADEM759>3.0.CO;2-A.
4. Wierzbicki, T. Crushing analysis of metal honeycomb. *Int. J. Impact Eng.* **1983**, *1*, 157–174.
5. Zhang, J.; Supernak, P.; Mueller-Alander, S.; Wang, C.H. Improving the bending strength and energy absorption of corrugated sandwich composite structure. *Mater. Des.* **2013**, *52*, 767–773, doi:10.1016/j.matdes.2013.05.018.
6. Torre, L.; Kenny, J.M. Impact testing and simulation of composite sandwich structures for civil transportation. *Compos. Struct.* **2000**, *50*, 257–267, doi:10.1016/S0263-8223(00)00101-X.
7. Shin, K.B.; Lee, J.Y.; Cho, S.H. An experimental study of low-velocity impact responses of sandwich panels for Korean low floor bus. *Compos. Struct.* **2008**, *84*, 228–240, doi:10.1016/j.compstruct.2007.08.002
8. Tan, X.; Chen, X. Parameters affecting energy absorption and deformation in textile composite cellular structures. *Mater. Des.* **2005**, *26*, 424–438, doi:10.1016/j.matdes.2004.07.013.
9. Roberts, J.C.; Boyle, M.P.; Wienhold, P.D.; White, G.J. Buckling, collapse and failure analysis of FRP sandwich panels. *Compos. Part B Eng.* **2002**, *33*, 315–324, doi:10.1016/S1359-8368(02)00017-3.
10. Shiah, Y.C.; Tseng, L.; Hsu, J.C.; Huang, J.H. Experimental Characterization of an Integrated Sandwich Composite Using 3D Woven Fabrics as the Core Material. *J. Thermoplast. Compos. Mater.* **2004**, *17*, 229–243, doi:10.1177/0892705704035410.
11. Shaw, M.C.; Sata, T. The plastic behavior of cellular materials. *Int. J. Mech. Sci.* **1966**, *8*, 469–478, doi:10.1016/0020-7403(66)90019-1.
12. Vaidya, U..; Hosur, M..; Earl, D.; Jeelani, S. Impact response of integrated hollow core sandwich composite panels. *Compos. Part A Appl. Sci. Manuf.* **2000**, *31*, 761–772, doi:10.1016/S1359-835X(00)00025-7.
13. Prall, D.; Lakes, R.S. Properties of a chiral honeycomb with a poisson’s ratio of — 1. *Int. J. Mech. Sci.* **1997**, *39*, 305–314, doi:10.1016/S0020-7403(96)00025-2.
14. Thwaites, S.; Clark, N.H. Non-destructive testing of honeycomb sandwich structures using elastic waves. *J. Sound Vib.* **1995**, *187*, 253–269, doi:10.1006/jsvi.1995.0519.
15. Aktay, L.; Çakıroğlu, C.; Güden, M. Quasi-Static Axial Crushing Behavior of Honeycomb-Filled Thin-Walled Aluminum Tubes. *Open Mater. Sci. J.* **2011**, *5*, 184–193, doi:10.2174/1874088X01105010184.
16. Gary, G.; Klepaczko, J.R. Quasi-static and impact tests of honeycomb. *J. Phys. IV* **2006**, *134*, 819–826, doi:10.1051/jp4:2006134126.
17. Zhang, X.W.; Yu, T.X. Energy absorption of pressurized thin-walled circular tubes under axial crushing. *Int. J. Mech. Sci.* **2009**, *51*, 335–349, doi:10.1016/j.ijmecsci.2009.03.002.
18. Kobayashi, H.; Daimaruya, M.; Kobayashi, T. Dynamic and Static Compression Tests for Paper Honeycomb Cores and Absorbed Energy. *JSME Int. J. Ser. A* **1998**, *41*, 338–344, doi:10.1299/jsmea.41.338.
19. Ashby, M.; Gibson, L. *Cellular solids*; Cambridge University Press, United Kingdom, 1997;
20. Dharmasena, K.P.; Queheillalt, D.T.; Wadley, H.N.G.; Dudt, P.; Chen, Y.; Knight, D.; Evans, A.G.; Deshpande, V.S. Dynamic compression of metallic sandwich structures during planar impulsive loading in water. *Eur. J. Mech. - A/Solids* **2010**, *29*, 56–67, doi:10.1016/j.euromechsol.2009.05.003.

21. Jiang, Q.; Chen, G.; Kumar, A.; Mills, A.; Jani, K.; Rajamohan, V.; Venugopal, B.; Rahatekar, S. Sustainable Sandwich Composites Manufactured from Recycled Carbon Fibers, Flax Fibers/PP Skins, and Recycled PET Core. *J. Compos. Sci.* **2020**, *5*, 2, doi:10.3390/jcs5010002.
22. Alsubari, S.; Zuhri, M.Y.M.; Sapuan, S.M.; Ishak, M.R.; Ilyas, R.A.; Asyraf, M.R.M. Potential of Natural Fiber Reinforced Polymer Composites in Sandwich Structures: A Review on Its Mechanical Properties. *Polymers (Basel).* **2021**, *13*, 423, doi:10.3390/polym13030423.
23. Gibson, L.J.; Ashby, M.F. *Cellular Solids: Structure and Properties, 2d ed*; 1997; ISBN 0521495601.
24. Tripathi, L.; Neje, G.; Behera, B.K. Geometrical modeling of 3D woven honeycomb fabric for manufacturing of lightweight sandwich composite material. *J. Ind. Text.* **2020**, 152808372093147, doi:10.1177/1528083720931472.
25. Tan, X.; Chen, X. Parameters affecting energy absorption and deformation in textile composite cellular structures. *Mater. Des.* **2005**, *26*, 424–438, doi:10.1016/j.matdes.2004.07.013.
26. Bitzer, T. *Honeycomb Technology: Materials, Design, Manufacturing, Applications And Testing*; 1997; ISBN 978-94-010-6474-3.